

NACA RM L9E25



RESEARCH MEMORANDUM

AERODYNAMIC CHARACTERISTICS OF A WING WITH QUARTER-
CHORD LINE SWEPT BACK 45° , ASPECT RATIO 4, TAPER
RATIO 0.3, AND NACA 65A006 AIRFOIL SECTION

TRANSONIC-BUMP METHOD

By

Boyd C. Myers, II, and Thomas J. King, Jr.

Langley Aeronautical Laboratory
Langley Air Force Base, Va.

CLASSIFICATION CANCELLED

CLASSIFIED DOCUMENT

Authority *NAAC R 7 2439* Date *8/18/54*

By *MDA 9/8/54* See

This document contains classified information affecting the National Defense of the United States within the meaning of the Espionage Act, Title 18, U.S.C., Sections 793 and 794. Its transmission or the revelation of its contents in any manner to an unauthorized person is prohibited by law. Information so classified may be imparted only to persons in the military and naval services of the United States, appropriate civilian officers and employees of the Federal Government who have a legitimate interest therein, and to United States citizens of known loyalty and discretion who of necessity must be informed thereof.

NATIONAL ADVISORY COMMITTEE
FOR AERONAUTICS

WASHINGTON
July 20, 1949

UNCLASSIFIED

~~CONFIDENTIAL~~



UNCLASSIFIED

NATIONAL ADVISORY COMMITTEE FOR AERONAUTICS

RESEARCH MEMORANDUM

AERODYNAMIC CHARACTERISTICS OF A WING WITH QUARTER-
CHORD LINE SWEPT BACK 45° , ASPECT RATIO 4, TAPER
RATIO 0.3, AND NACA 65A006 AIRFOIL SECTION

TRANSONIC-BUMP METHOD

By Boyd C. Myers, II, and Thomas J. King, Jr.

SUMMARY

As part of a transonic research program, a series of wing-body combinations are being investigated in the Langley high-speed 7-by 10-foot tunnel over a Mach number range of about 0.60 to 1.18 utilizing the transonic-bump test technique.

This paper presents the results of the investigation of a wing-alone and wing-fuselage configuration employing a wing with the quarter-chord line swept back 45° , with aspect ratio 4, taper ratio 0.3, and an NACA 65A006 airfoil section. Lift, drag, pitching moment, and root bending moment were obtained for these configurations. In addition, effective downwash angles and dynamic-pressure characteristics in the region of a probable tail location were also obtained for these configurations and are presented for a range of tail heights at one tail length. In order to expedite the publishing of these data, only a brief analysis is included.

INTRODUCTION

A series of wings with and without a body are being investigated in the Langley high-speed 7-by 10-foot tunnel to study the effects of wing geometry on the longitudinal stability characteristics at transonic speeds. A Mach number range between 0.60 and 1.18 is obtained utilizing the transonic-bump technique. Previous data published in this series are presented in references 1 and 2.

~~CONFIDENTIAL~~

UNCLASSIFIED

This paper presents the results of the investigation of the wing-alone and wing-fuselage configurations employing a wing with the quarter-chord line swept back 45° , aspect ratio 4, taper ratio 0.3, and an NACA 65A006 airfoil section parallel to the stream.

MODEL AND APPARATUS

The wing of the semispan model had 45° of sweepback referred to the quarter-chord line, aspect ratio 4, taper ratio 0.3, and an NACA 65A006 airfoil section parallel to the free stream. The wing was made of beryllium copper and the fuselage of brass. A two-view drawing of the model is presented in figure 1, while ordinates of the fuselage of fineness ratio 10 are given in table I.

The model was mounted on an electrical strain-gage balance, which was enclosed in the bump; and the lift, drag, pitching moment, and bending moment about the model plane of symmetry were measured with calibrated galvanometers.

Effective downwash angles were determined for a range of tail heights by measuring the floating angles of five free-floating tails with the aid of calibrated slide-wire potentiometers. Details of the floating tails are shown in figures 2 and 3, while a pictorial view of the model on the bump with three of the floating tails is given as figure 4. The tails used in this investigation were the same as those used in references 1 and 2.

A total-head comb was used to determine dynamic-pressure ratios for a range of tail heights in a plane which contained the 25-percent mean-aerodynamic-chord point of the free-floating tails. The total-head tubes were spaced 0.25 inch apart.

COEFFICIENTS AND SYMBOLS

C_L	lift coefficient $\left(\frac{\text{Twice panel lift}}{qS} \right)$
C_D	drag coefficient $\left(\frac{\text{Twice panel drag}}{qS} \right)$
C_m	pitching-moment coefficient referred to 0.25c $\left(\frac{\text{Twice panel pitching moment}}{qS\bar{c}} \right)$

C_B	bending-moment coefficient at plane of symmetry $\left(\frac{\text{Root bending moment}}{q \frac{S}{2} \frac{b}{2}} \right)$
q	effective dynamic pressure over span of model, pounds per square foot $\left(\frac{1}{2} \rho V^2 \right)$
S	twice wing area of semispan model, 0.125 square foot
\bar{c}	mean aerodynamic chord of wing, 0.181 foot; based on relationship $\frac{2}{S} \int_0^{b/2} c^2 dy$ (using theoretical tip)
c	local wing chord
b	twice span of semispan model
y	spanwise distance from plane of symmetry
ρ	air density, slugs per cubic foot
V	free-stream velocity, feet per second
M	effective-Mach number over span of model
M_L	local Mach number
M_a	average chordwise local Mach number
R	Reynolds number of wing based on \bar{c}
α	angle of attack, degrees
ϵ	effective downwash angle, degrees
q_{wake}/q	ratio of point dynamic pressure at the quarter chord of the tail mean aerodynamic chord to free-stream dynamic pressure
$y_{c.p.}$	lateral center of pressure, percent semispan $\left(100 \frac{C_B}{C_L} \right)$
h_t	tail height relative to wing chord plane extended, percent semispan; positive for tail positions above chord plane extended
a.c.	aerodynamic center

TESTS

The tests were made in the Langley high-speed 7- by 10-foot tunnel utilizing an adaptation of the NACA wing-flow technique for obtaining transonic speeds. The technique used involves the mounting of a model in the high-velocity flow field generated over the curved surface of a bump located on the tunnel floor. (See reference 3.)

Typical contours of local Mach number in the vicinity of the model location on the bump, obtained from surveys with no model in position, are shown in figure 5. It is seen that there is a Mach number gradient of about 0.04 over the model semispan at low Mach numbers and from 0.06 to 0.07 at the highest Mach numbers. The chordwise Mach number gradient is generally less than 0.01. No attempt has been made to evaluate the effects of the chordwise and spanwise Mach number variations. Note that the long dashed lines shown near the root of the wing (fig. 5) represent a local Mach number that is 5 percent below the maximum value and indicate the extent of the bump boundary layer. The effective test Mach number was obtained from contour charts similar to those presented in figure 5 using the relationship

$$M = \frac{2}{S} \int_0^{b/2} cM_a dy$$

The variation of mean test Reynolds number with Mach number is shown in figure 6. The boundaries on the figure indicate the range in Reynolds number caused by variations in test conditions in the course of the investigation.

Force and moment data, effective downwash angles, and the ratio of dynamic pressure at 25 percent of the mean aerodynamic chord of the tail to free-stream dynamic pressure were obtained for the model configurations tested through a Mach number range of 0.70 to 1.18 and an angle-of-attack range of -2° to 10° .

No tares have been applied to the data to account for the presence of the end plates on the models. Jet-boundary corrections have not been evaluated because the boundary conditions to be satisfied are not rigorously defined. However, inasmuch as the effective flow field is large compared with the span and chord of the model, these corrections are believed to be small.

By measuring tail floating angles without a model installed, it was determined that a tail spacing of 2 inches would produce negligible interference effects of reflected shock waves on the tail floating

angles. Downwash angles for the wing-alone configuration were therefore obtained simultaneously for the middle, highest, and lowest tail positions in one series of tests, and simultaneously for the two intermediate positions in succeeding runs. (See fig. 3.) For the wing-fuselage tests, the effective downwash angles at the chord-plane extended were determined by mounting a free-floating tail on the center line of the fuselage. The downwash angles presented are increments from the tail floating angles without a model in position. It should be noted that the floating angles measured are in reality a measure of the angle of zero pitching moment about the tail-pivot axis rather than the angle of zero lift. It has been estimated that, for the tail arrangement used, a downwash gradient of 2° across the span of the tail will result in an error of less than 0.2° in the measured downwash angle.

Total-head readings obtained from the tail-survey comb have been corrected for bow-wave loss. The static-pressure values used in computing dynamic-pressure ratios were obtained by use of a static probe with no model in position.

RESULTS AND DISCUSSION

A table of the figures presenting the results is given below:

	Figure
Wing-alone force data	7
Wing-fuselage force data	8
Effective downwash angles (wing alone)	9
Effective downwash angles (wing fuselage)	10
Downwash gradients	11
Dynamic-pressure surveys	12
Summary of aerodynamic characteristics	13

The discussion is based on the summarized values given in figure 13 unless otherwise noted. Note that the slopes summarized in figure 13 have been averaged over a lift-coefficient range of ± 0.1 at the given lift coefficient.

Lift and drag characteristics.— The isolated wing lift-curve slope measured near zero lift was about 0.064 at a Mach number of 0.70. This slope compares with a value of 0.065 estimated for this Mach number using unpublished semispan data for a geometrically similar model from the Langley two-dimensional tunnel as a low-speed point and applying a compressibility correction as outlined in reference 4. The basic

lift-curve slope up to a Mach number of 1.00 was increased about 10 percent by the addition of the fuselage. Beyond a Mach number of 1.00 the fuselage effect on the lift-curve slope is diminished.

The drag rise at zero lift began at a Mach number of about 0.93 for both the wing-alone and wing-fuselage configurations. The drag characteristics are very similar to those obtained for the wing of reference 1, which, except for taper ratio, had identical geometric characteristics as the present wing. The absolute drag coefficients are probably high because of the presence of the end plates and the relatively low Reynolds numbers at which these tests were made.

The lateral center of pressure for the wing alone ($C_L = 0.4$) was located at 45 percent of the semispan at a Mach number of 0.70. This center-of-pressure location compares with a value of 44 percent semispan obtained from the unpublished low-speed data from the Langley two-dimensional tunnel at a Reynolds number of 12×10^6 . Between $M = 0.85$ and 0.95 there was a fairly abrupt movement of $y_{c.p.}$ to about 49 percent semispan. In a Mach number range from 0.95 to 1.05, an outboard shift of about the same magnitude was obtained with the less tapered 45° sweptback wing (reference 1). The addition of the fuselage moved the lateral center of pressure inboard about 2 percent of the semispan at low Mach numbers and there was very little outboard shift through the Mach number range.

Pitching-moment characteristics.- Near zero lift the wing-alone aerodynamic center was located at 40 percent of the mean aerodynamic chord $\left(\left(\frac{\partial C_M}{\partial C_L} \right)_M = -0.15 \right)$ up to $M = 0.90$. This value compares with a value of 36 percent of the mean aerodynamic chord obtained from unpublished low-speed two-dimensional-tunnel data for this wing. The addition of the fuselage moved the aerodynamic center rearward about 1 percent mean aerodynamic chord at low Mach numbers but is generally about 5 percent destabilizing above a Mach number of 0.95.

In the subsonic speed range, the wing-alone and wing-fuselage pitching-moment curves indicate instability at the higher lift coefficients. (See figs. 7 and 8.) It is interesting to note, however, that above $M = 1.03$ there is no indication of this unstable trend even at the highest lift coefficient attained ($C_L \approx 0.6$). Similar trends were observed for the sweptback wing configurations reported in references 1 and 2.

Downwash and dynamic-pressure surveys.- At Mach numbers below 1.00, the downwash gradient $\partial \epsilon / \partial \alpha$ near zero lift for the wing alone (fig. 11) increased as the tail location approached the chord plane.

Above $M = 1.00$, the value of $\partial \epsilon / \partial \alpha$ was generally a maximum at tail locations about 35 percent above the chord plane. At higher lift coefficients $\partial \epsilon / \partial \alpha$ was generally lower than the zero-lift values for tail positions below the chord plane and was higher for tail positions above the chord plane (fig. 9).

The addition of the fuselage generally had little effect on $\partial \epsilon / \partial \alpha$ throughout the Mach number range for practically all tail heights. Note that the test angle-of-attack range with the free-floating tails nearest the chord line extended was restricted because of the presence of the fuselage (fig. 10).

The results of the point dynamic-pressure surveys made in a vertical plane containing the 25-percent mean-aerodynamic-chord point of the free-floating tails used in the downwash surveys are presented in figure 12. The maximum loss in dynamic pressure at the wake center line for $\alpha = 10^\circ$ was 18 percent of the free-stream dynamic pressure at the highest Mach number.

The addition of the fuselage had little or no effect on the dynamic-pressure ratios throughout most of the Mach number range. At $\alpha = 10^\circ$ the center line of the wake was located at a tail height of 7 percent semispan throughout the Mach number range.

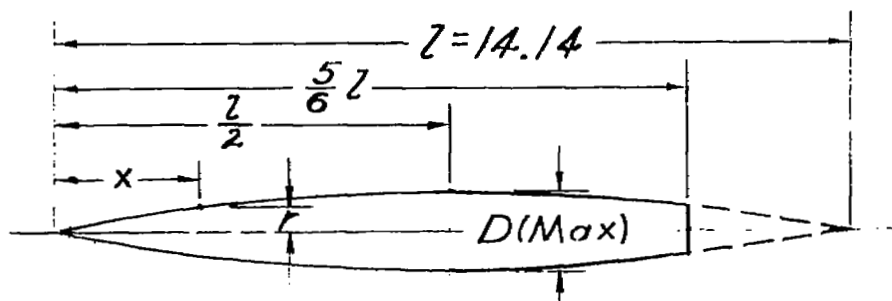
Langley Aeronautical Laboratory
National Advisory Committee for Aeronautics
Langley Air Force Base, Va.

REFERENCES

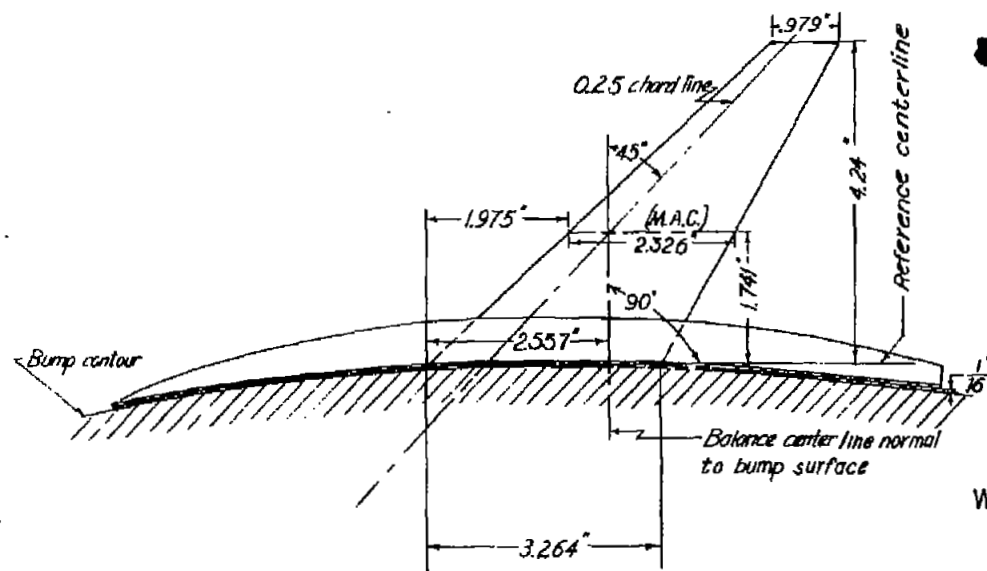
1. Weil, Joseph, and Goodson, Kenneth W.: Aerodynamic Characteristics of a Wing with Quarter-Chord Line Swept Back 45° , Aspect Ratio 4, Taper Ratio 0.6, and NACA 65A006 Airfoil Section. Transonic-Bump Method. NACA RM No. L9A21, 1949.
2. Sleeman, William C., Jr., and Becht, Robert E.: Aerodynamic Characteristics of a Wing with Quarter-Chord Line Swept Back 35° , Aspect Ratio 4, Taper Ratio 0.6, and NACA 65A006 Airfoil Section. Transonic-Bump Method. NACA RM No. L9B25, 1949.
3. Schneider, Leslie E., and Ziff, Howard L.: Preliminary Investigation of Spoiler Lateral Control on a 42° Sweptback Wing at Transonic Speeds. NACA RM No. L7F19, 1947.
4. DeYoung, John: Theoretical Additional Span Loading Characteristics of Wings with Arbitrary Sweep, Aspect Ratio, and Taper Ratio. NACA TN No. 1491, 1947.

TABLE I.- FUSELAGE ORDINATES

[Basic fineness ratio 12; actual fineness ratio 10
achieved by cutting off the rear one-sixth of
the body; $\bar{c}/4$ located at $l/2$]

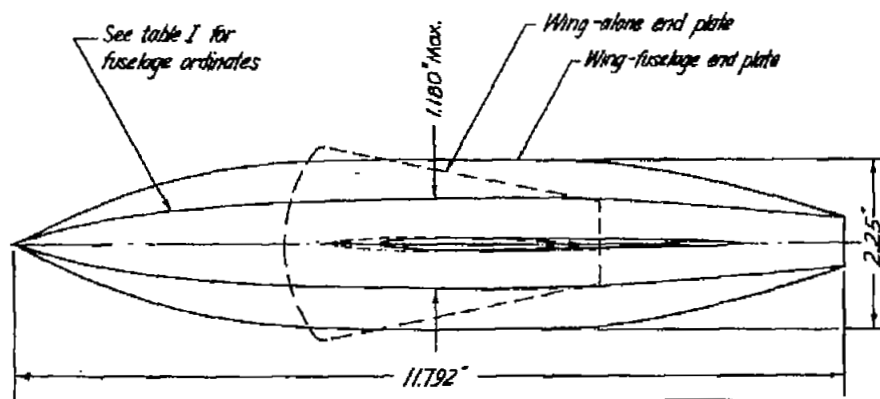


Ordinates			
x/l	r/l	x/l	r/l
0	0	0	0
.005	.00231	.4500	.04143
.0075	.00298	.5000	.04167
.0125	.00428	.5500	.04130
.0250	.00722	.6000	.04024
.0500	.01205	.6500	.03842
.0750	.01613	.7000	.03562
.1000	.01971	.7500	.03128
.1500	.02593	.8000	.02526
.2000	.03090	.8338	.02000
.2500	.03465	.8500	.01852
.3000	.03741	.9000	.01125
.3500	.03933	.9500	.00439
.4000	.04063	1.0000	0
L. E. radius = 0.00057			



WING DATA

Twice semispan area	0.125 sq ft
Aspect ratio	4.0
Taper ratio	0.3
Airfoil section parallel to air stream	NACA 65A006
M.A.C.	0.1938 ft
Dihedral	0°
Incidence	0°



Scale, inches

Figure 1.- General arrangement of model with 45° sweptback wing, aspect ratio 4, taper ratio 0.3, and NACA 65A006 airfoil.

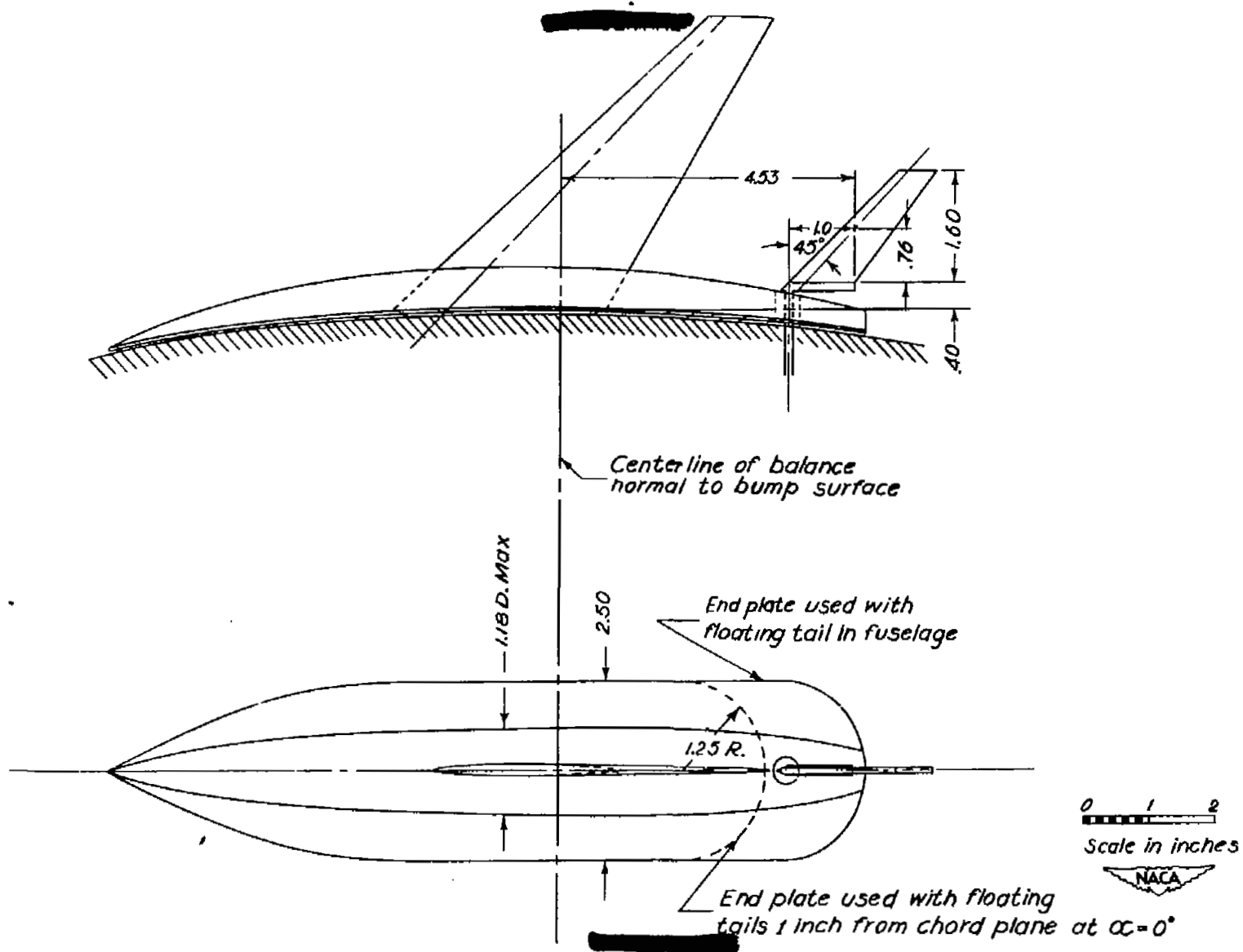


Figure 2.- Details of free-floating tails mounted on model with 45° sweptback wing, aspect ratio 4, taper ratio 0.3, and NACA 65A006 airfoil.

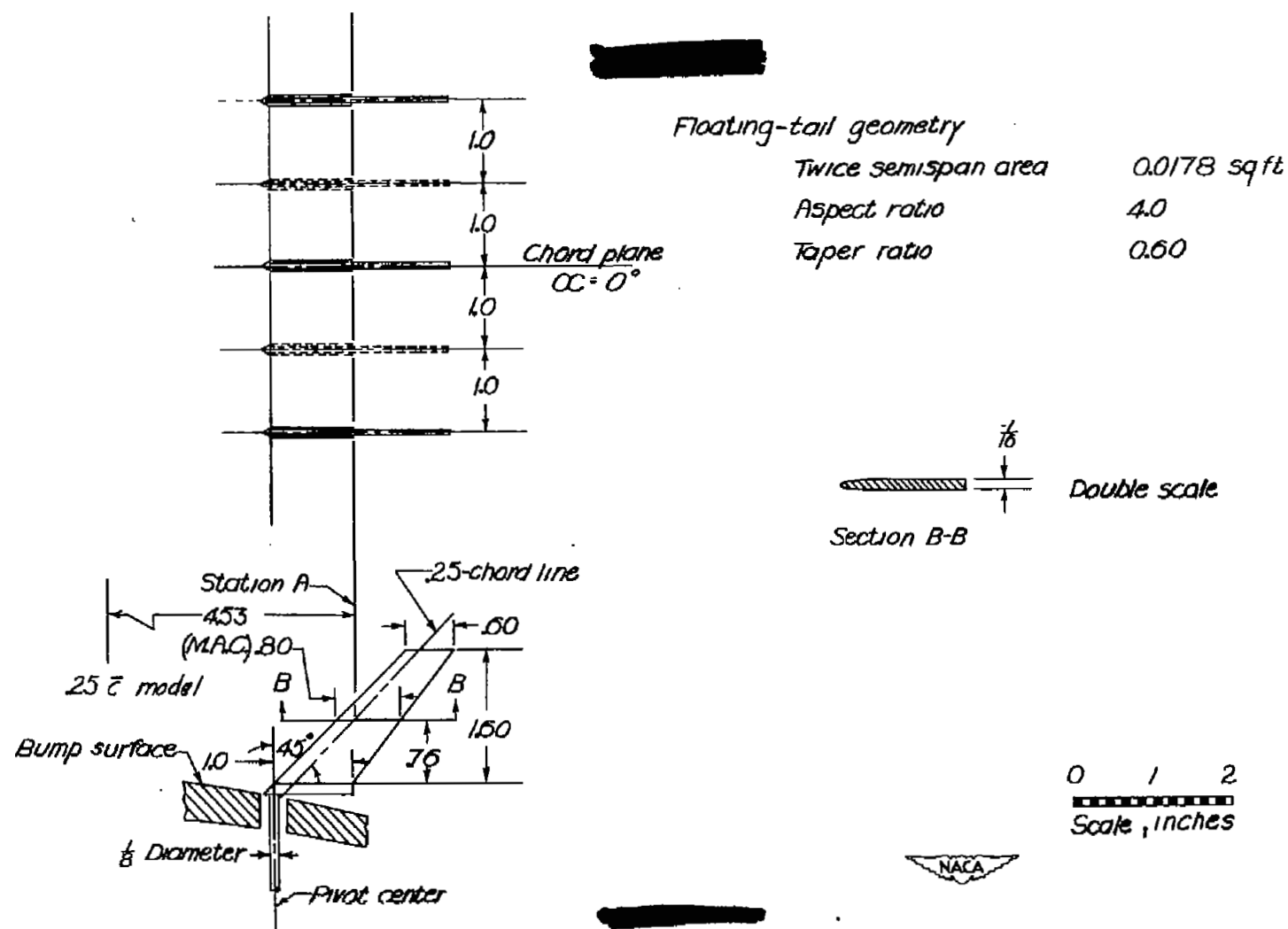


Figure 3.- Details of free-floating tails used in surveys behind model with 45° sweptback wing, aspect ratio 4, taper ratio 0.3, and NACA 65A006 airfoil.

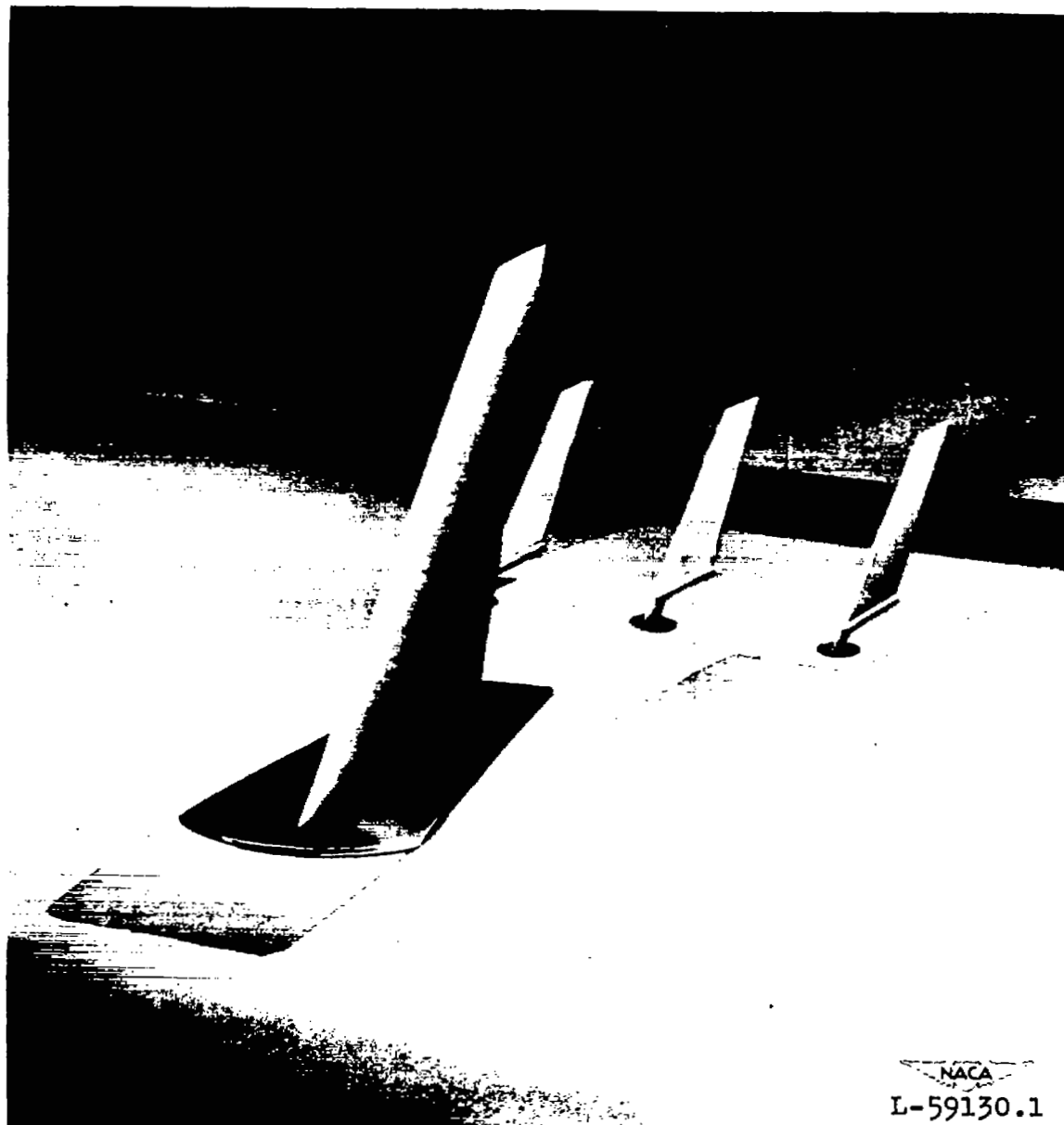


Figure 4.- Model mounted on the bump with three free-floating tails installed. Wing-alone configuration.

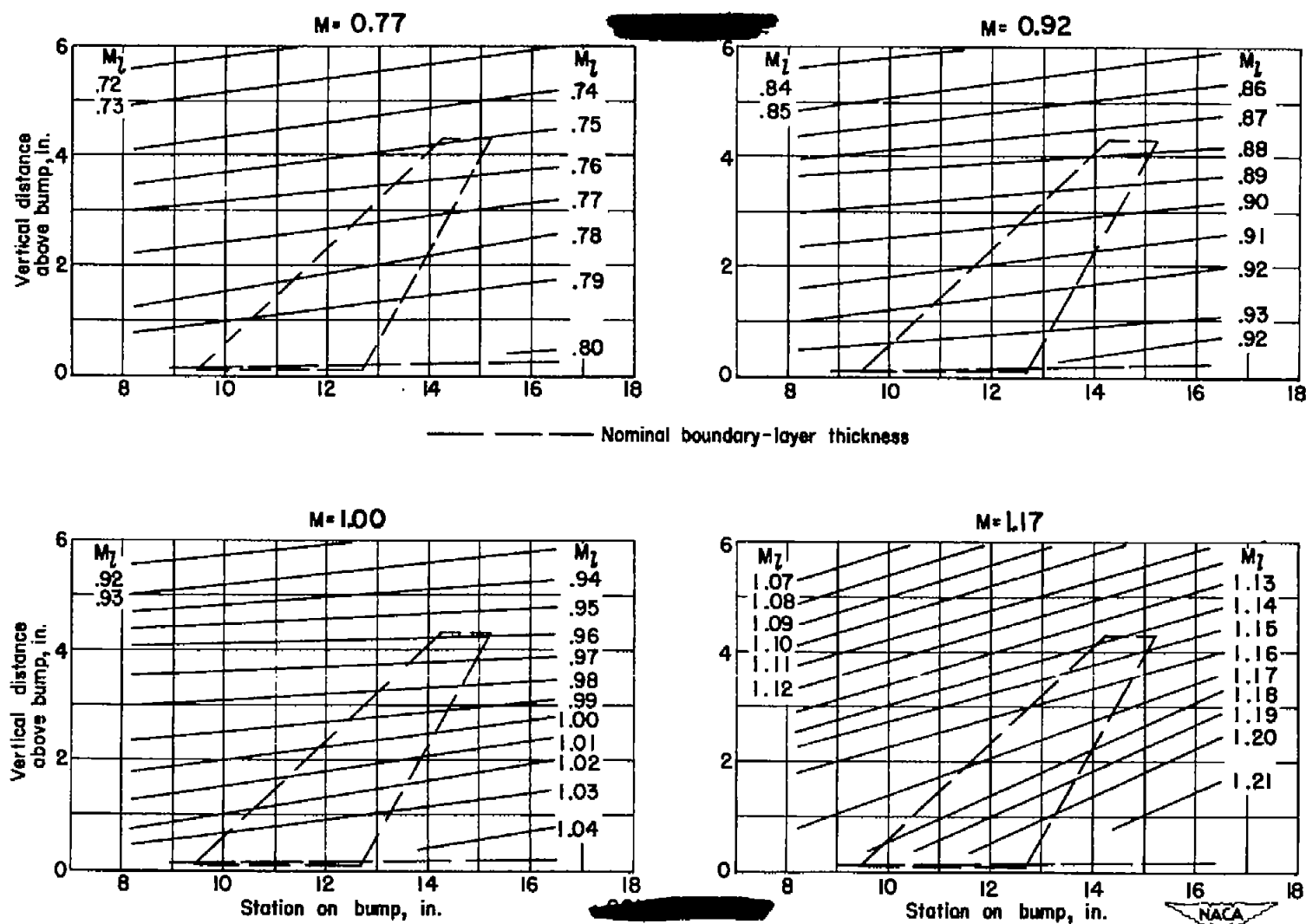


Figure 5.- Typical Mach number contours over transonic bump in region of model location.

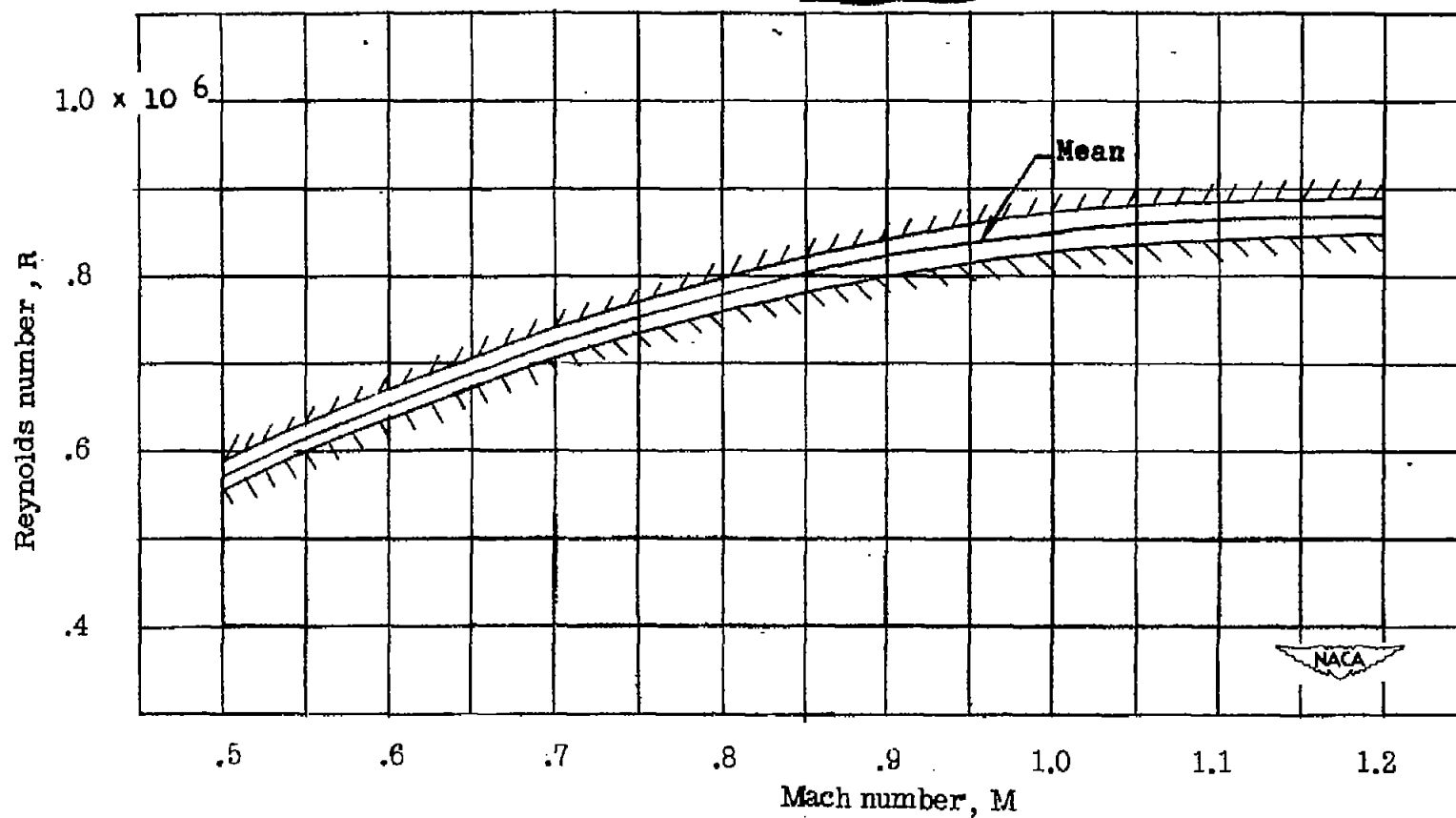


Figure 6.-- Variation of test Reynolds number with Mach number for model with 45° sweptback wing, aspect ratio 4, taper ratio 0.3, and NACA 65A006 airfoil.

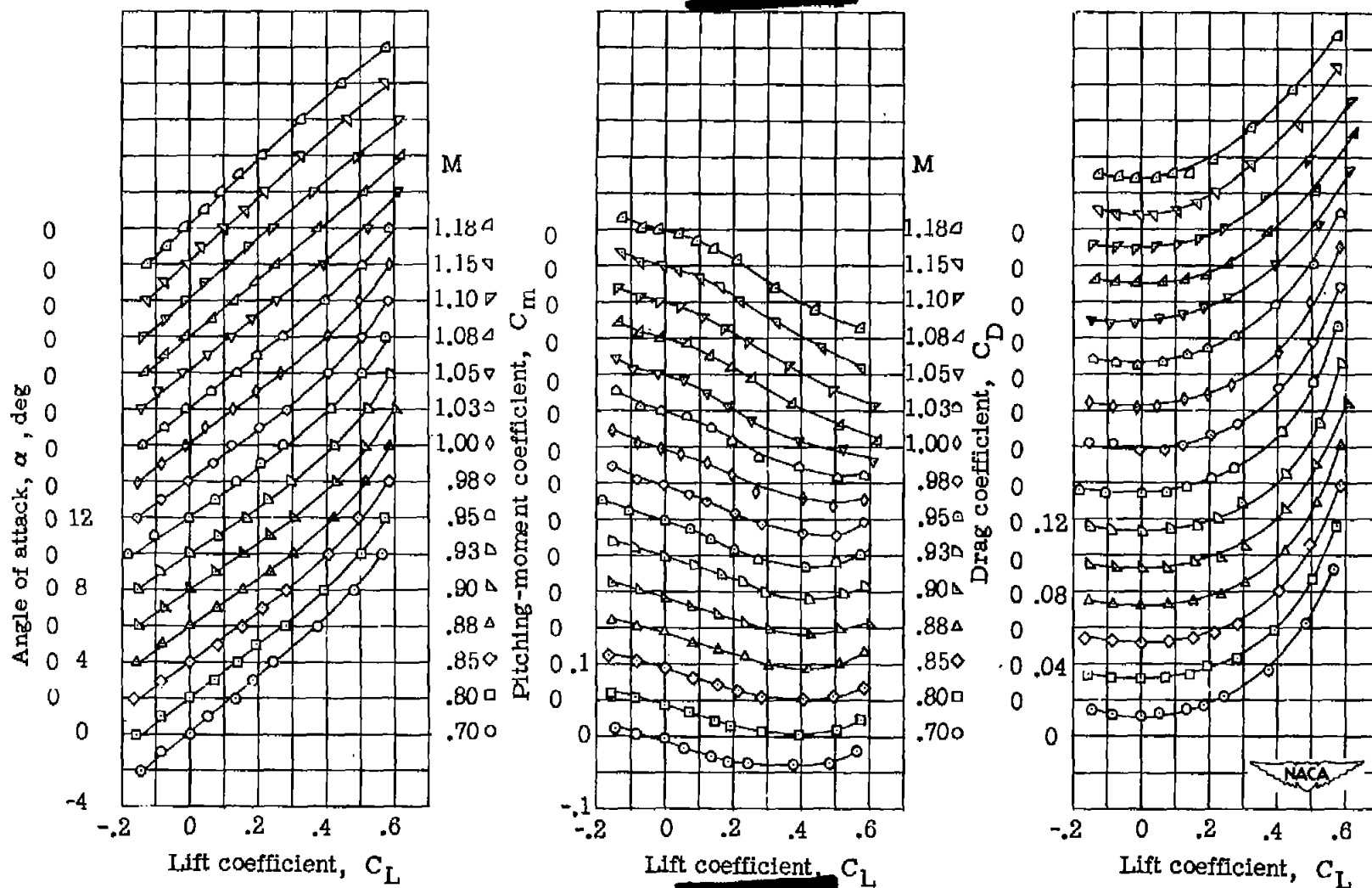


Figure 7.- Wing-alone aerodynamic characteristics for model with 45° sweptback wing, aspect ratio 4, taper ratio 0.3, and NACA 65A006 airfoil.

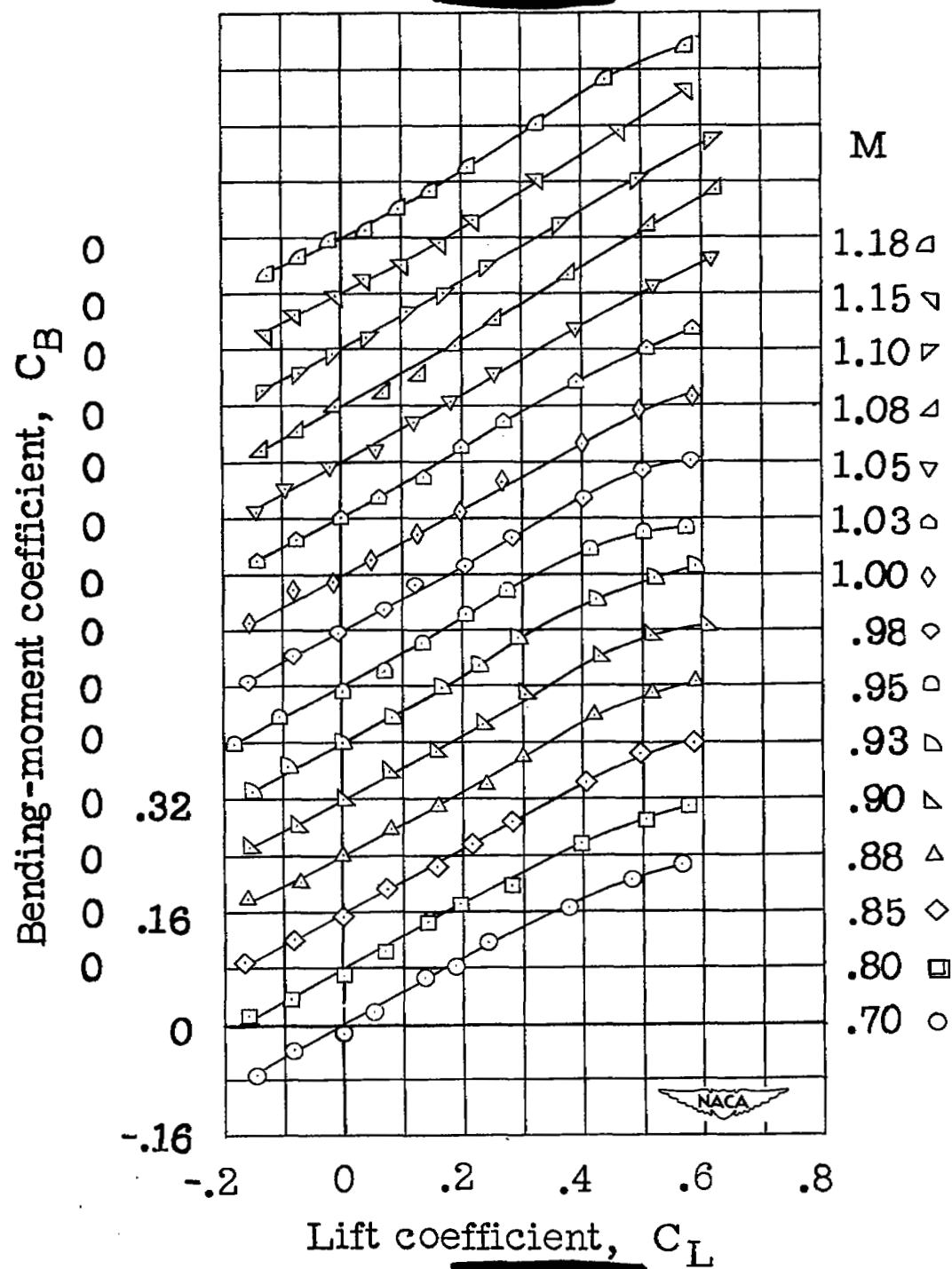


Figure 7.- Concluded.

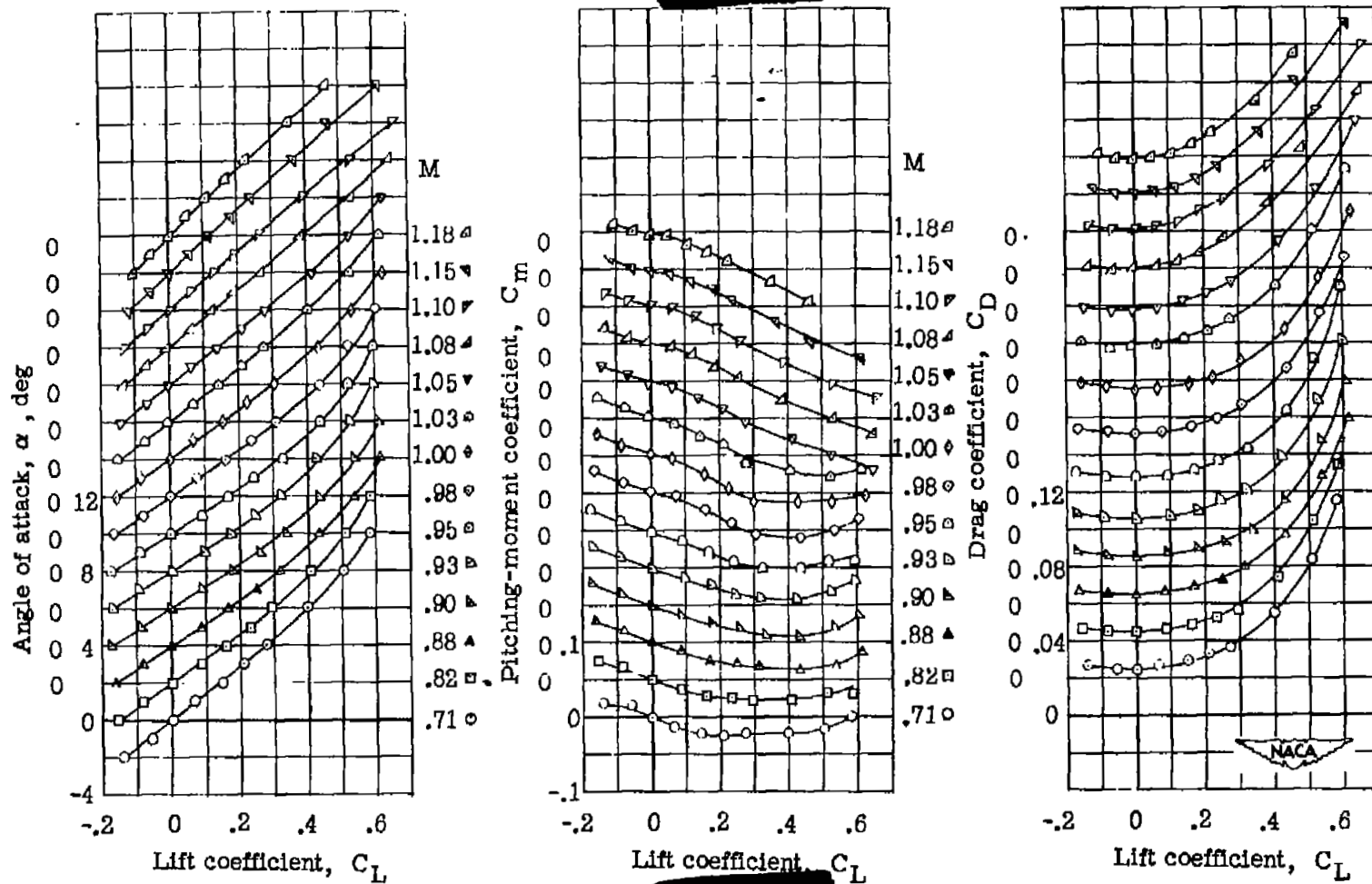


Figure 8.- Wing-fuselage aerodynamic characteristics for model with 45° sweptback wing, aspect ratio 4, taper ratio 0.3, and NACA 65A006 airfoil.

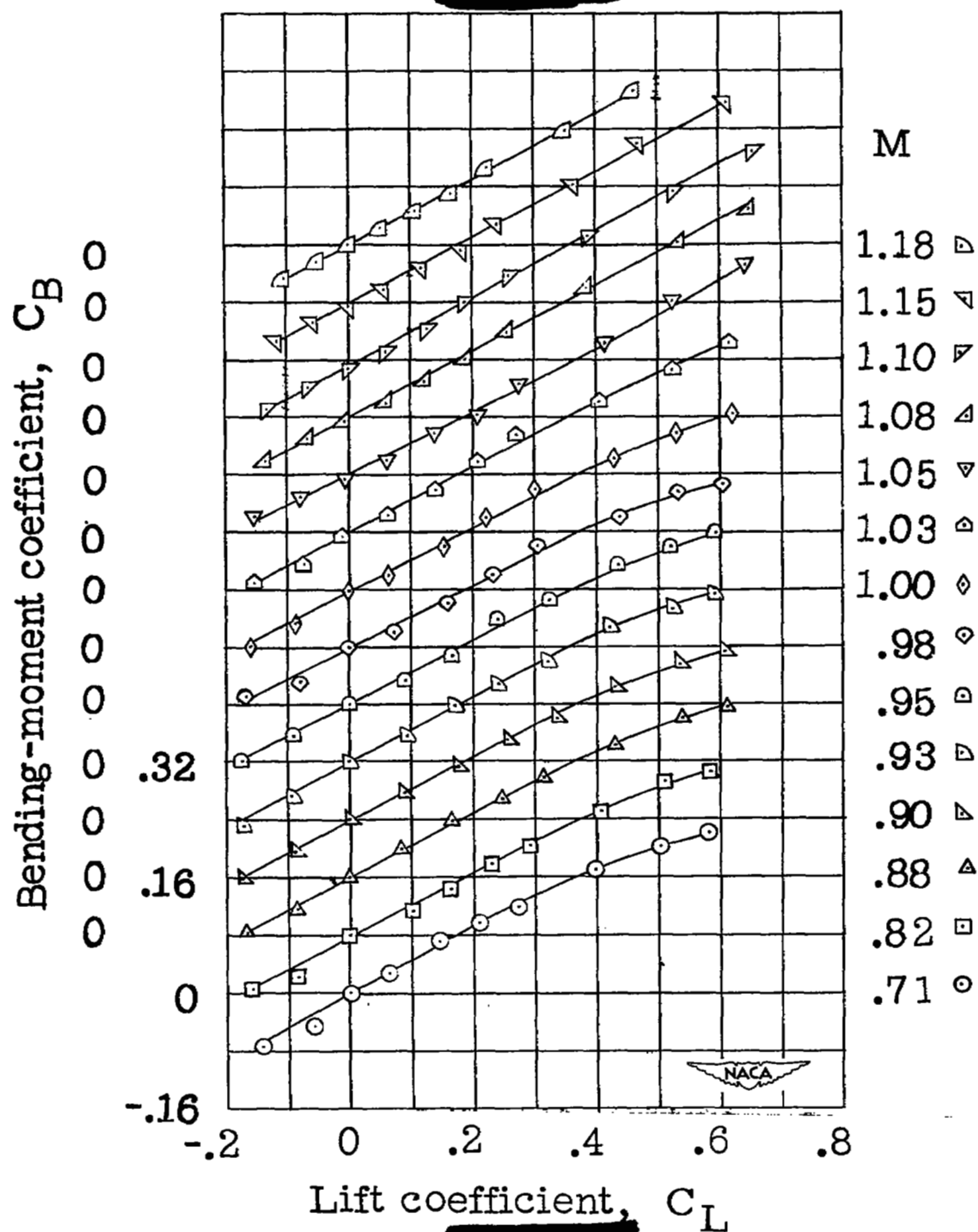
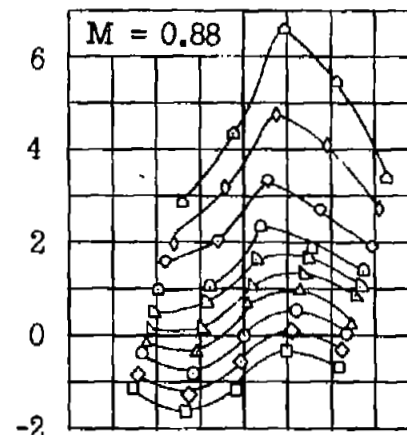
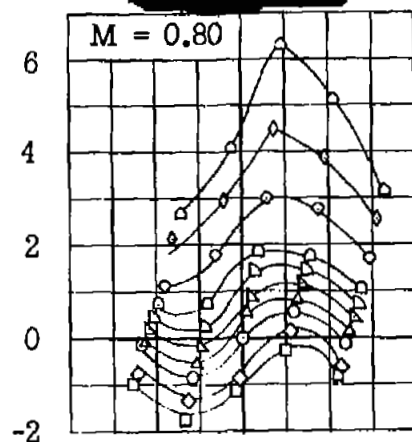
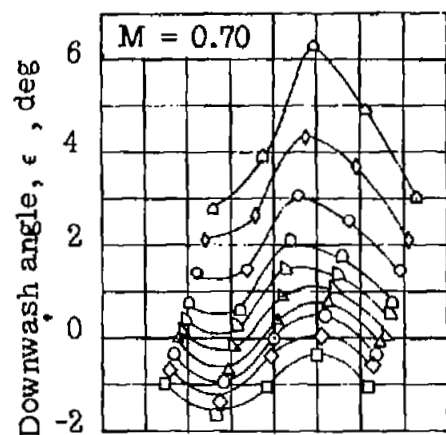


Figure 8.- Concluded.



α , deg -2, -1, 0, 1, 2, 3, 4, 6, 8, 10
 Symbol \square \diamond \circ \triangle ∇ \square \diamond \circ \triangle ∇

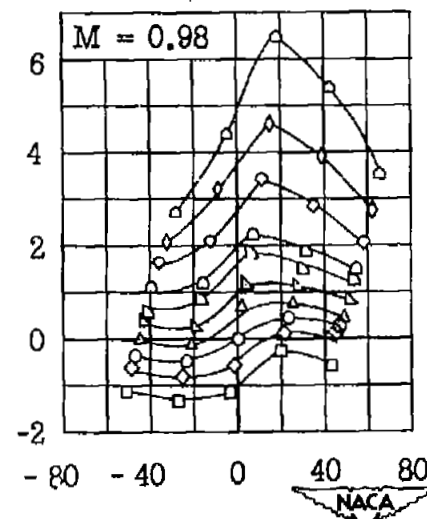
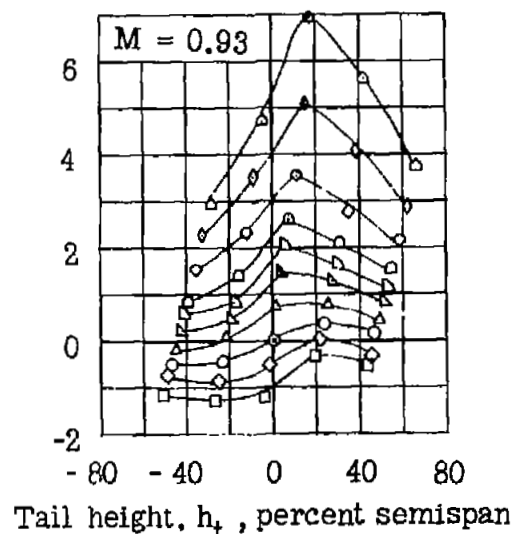
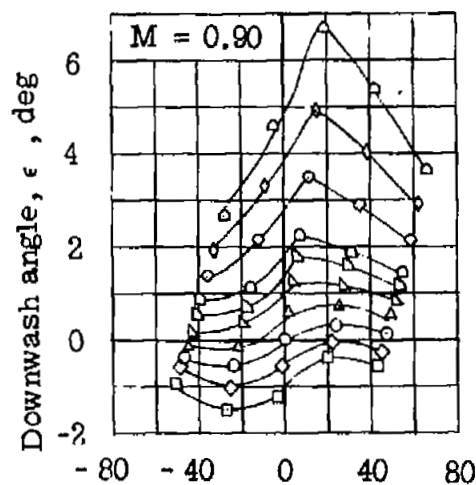
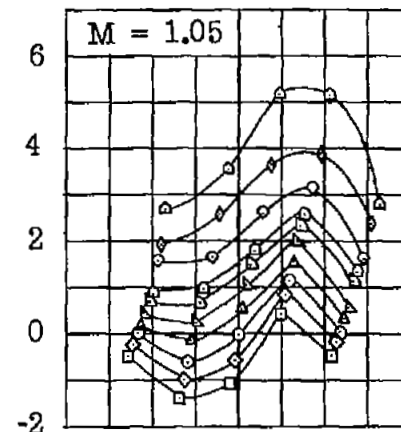
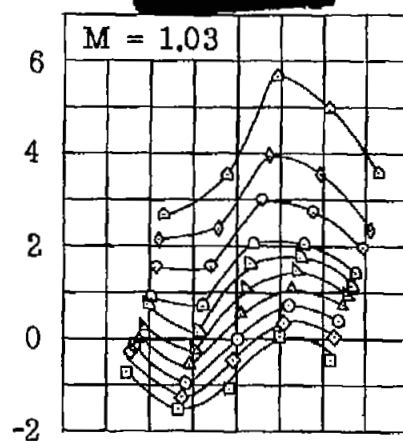
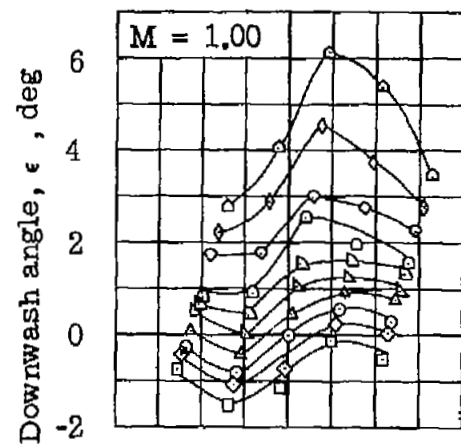
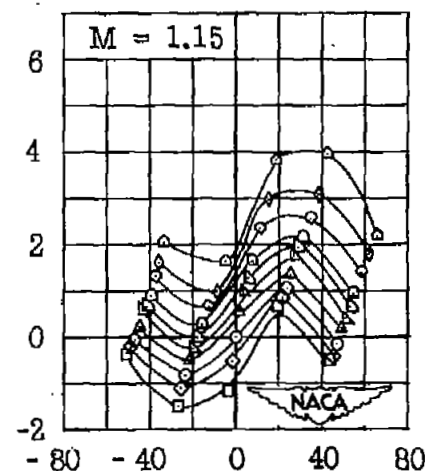
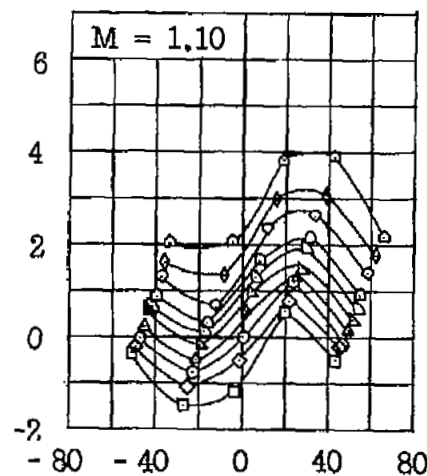
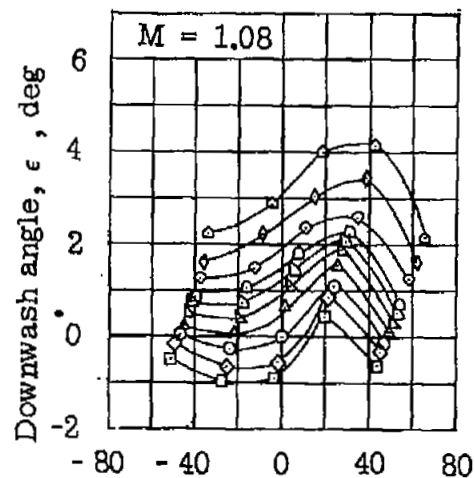


Figure 9.- Effective downwash angles in region of tail plane for a model with 45° sweptback wing, aspect ratio 4, taper ratio 0.3, and NACA 65A006 airfoil. Wing alone.



α , deg -2, -1, 0, 1, 2, 3, 4, 6, 8, 10
 Symbol \square \diamond \circ \triangle ∇ \square \diamond \circ \triangle



Tail height, h_t , percent semispan

Figure 9.- Concluded.

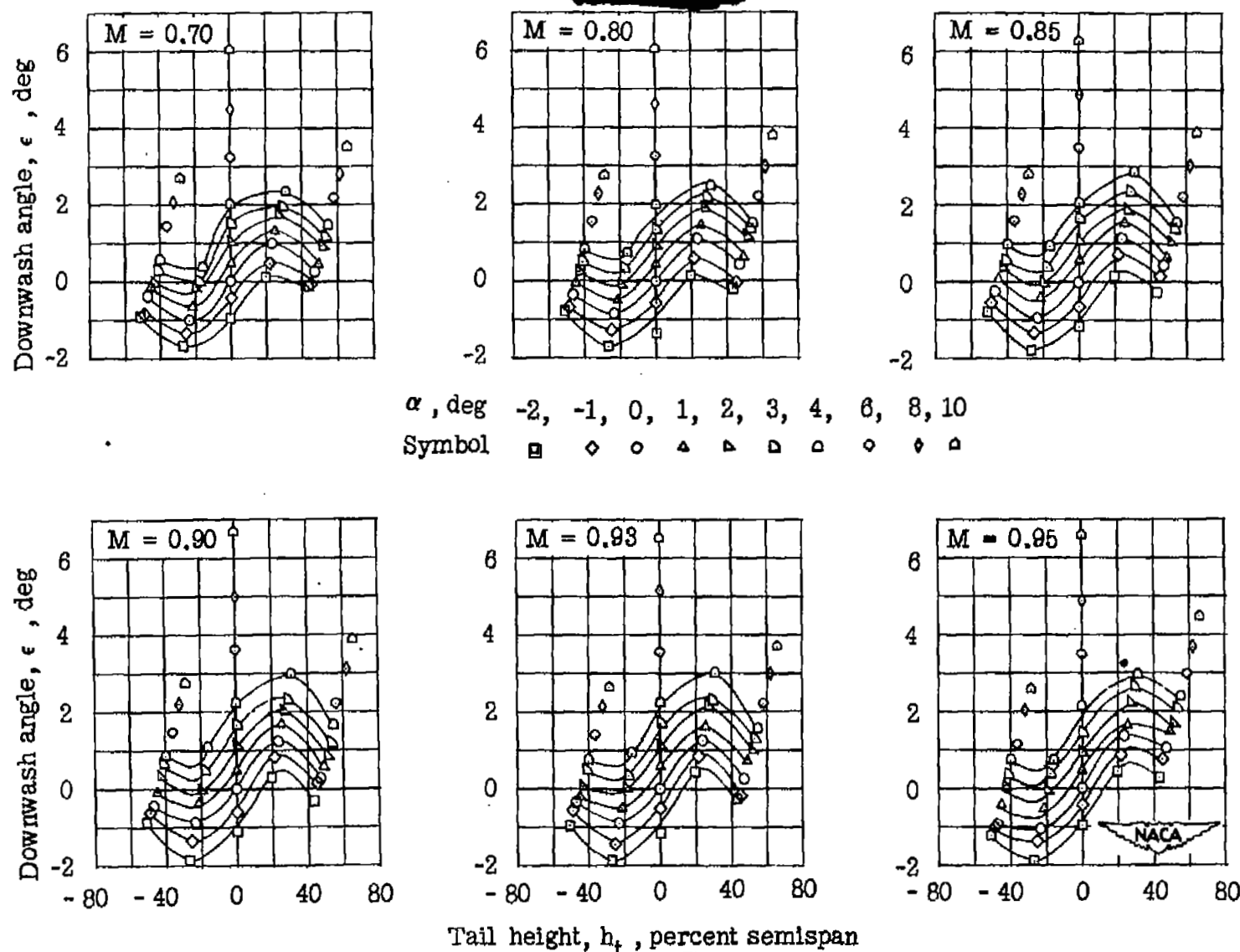
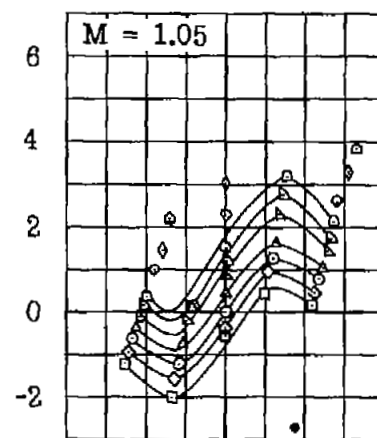
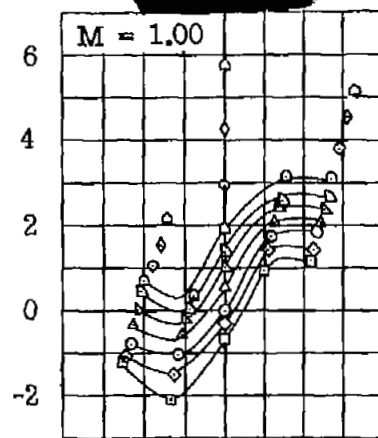
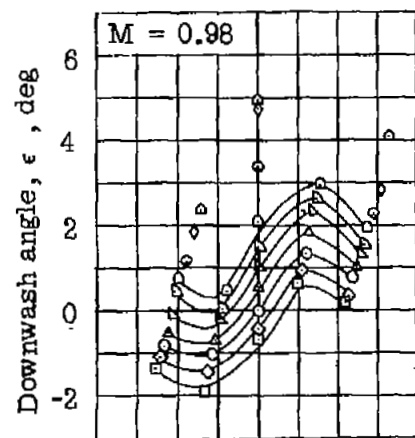
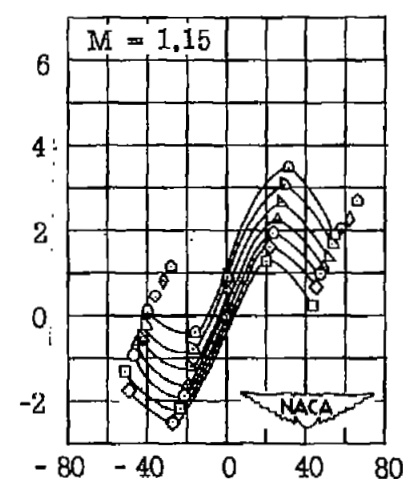
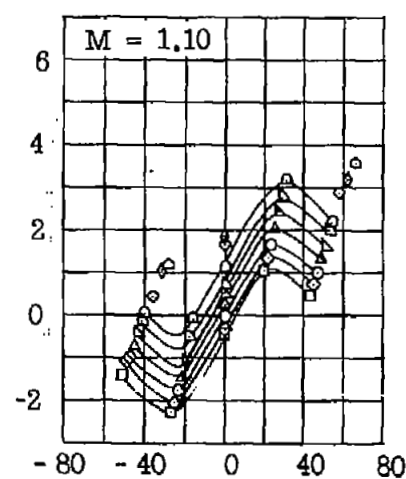
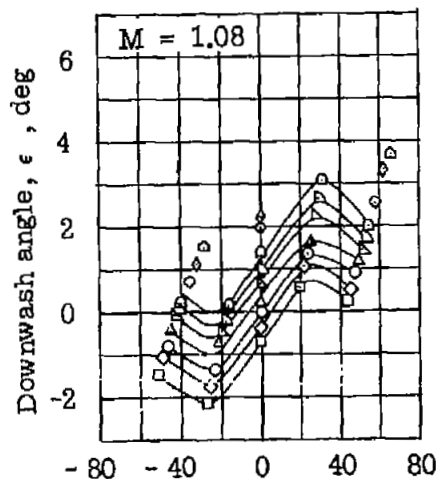


Figure 10.- Effective downwash angles in region of tail plane for a model with 45° sweptback wing, aspect ratio 4, taper ratio 0.3, and NACA 65A006 airfoil. Wing fuselage.



α , deg
Symbol

-2, -1, 0, 1, 2, 3, 4, 6, 8, 10
□ ◇ ○ △ ▽ ▹ ▸ ○ ◇



Tail height, h_t , percent semispan

Figure 10.- Concluded.

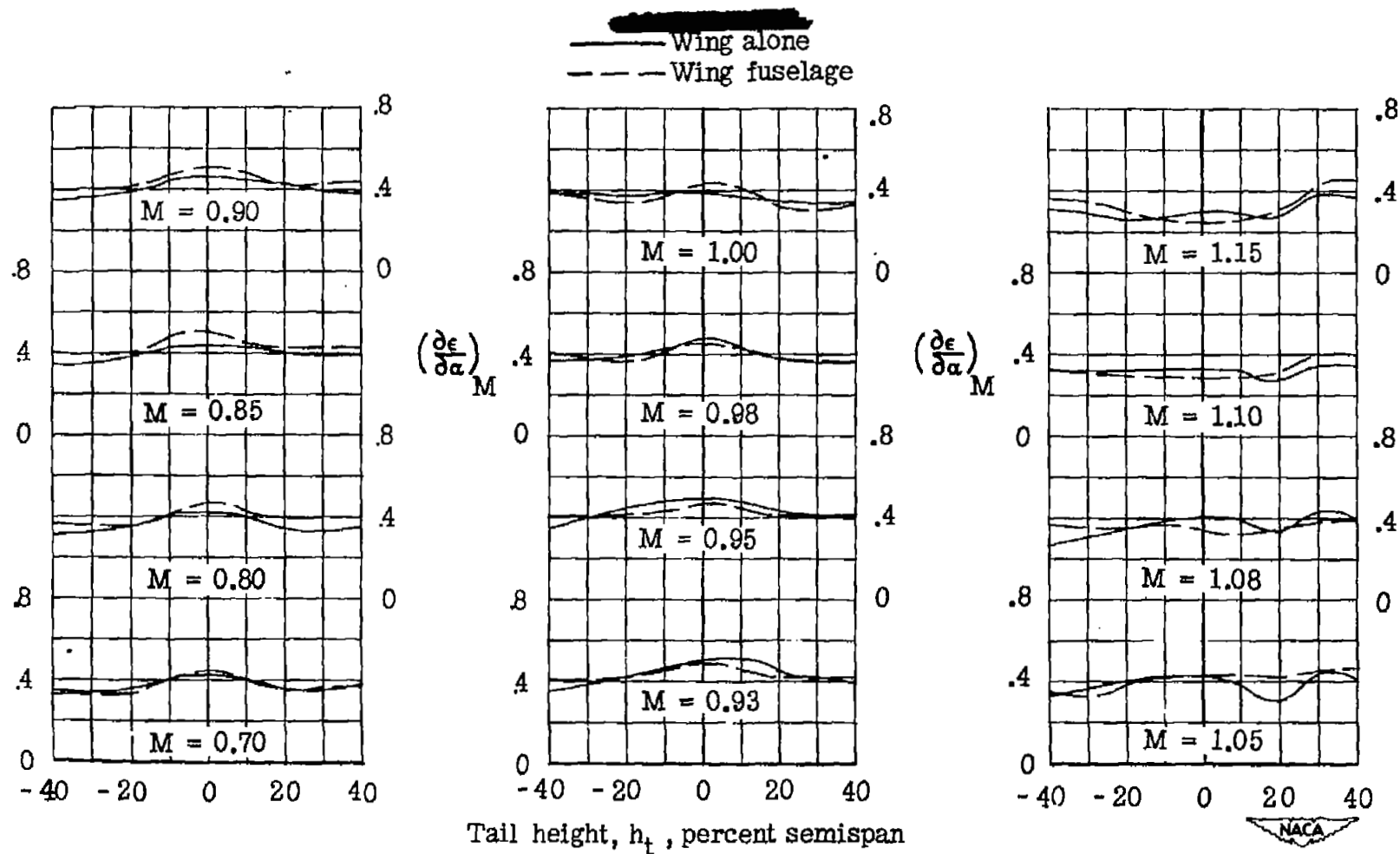


Figure 11.- Variation of downwash gradient with tail height for a model with 45° sweptback wing, aspect ratio 4, taper ratio 0.3, and NACA 65A006 airfoil.

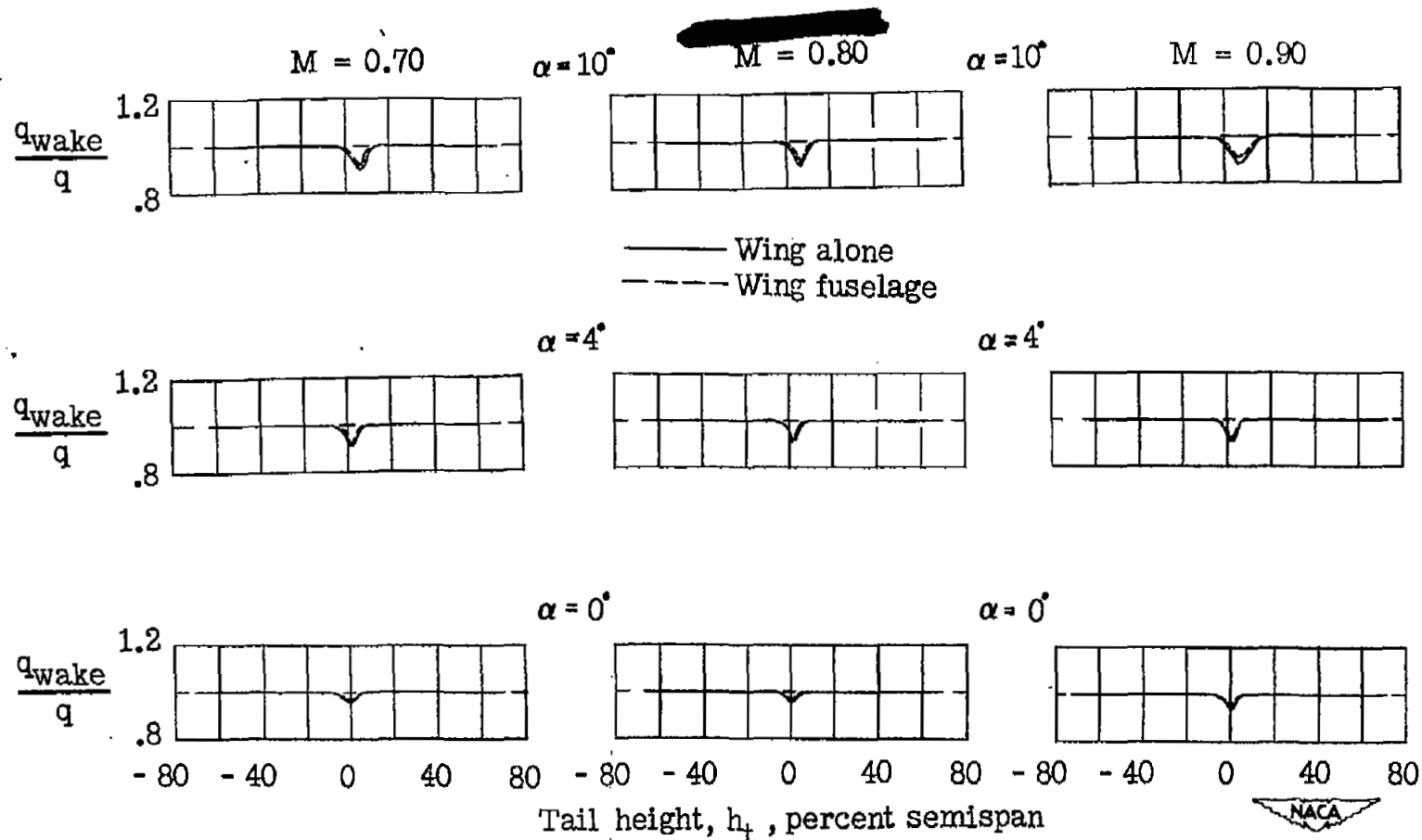


Figure 12.- Dynamic pressure surveys in region of tail plane for a model with 45° sweptback wing, aspect ratio 4, taper ratio 0.3, and NACA 65A006 airfoil.

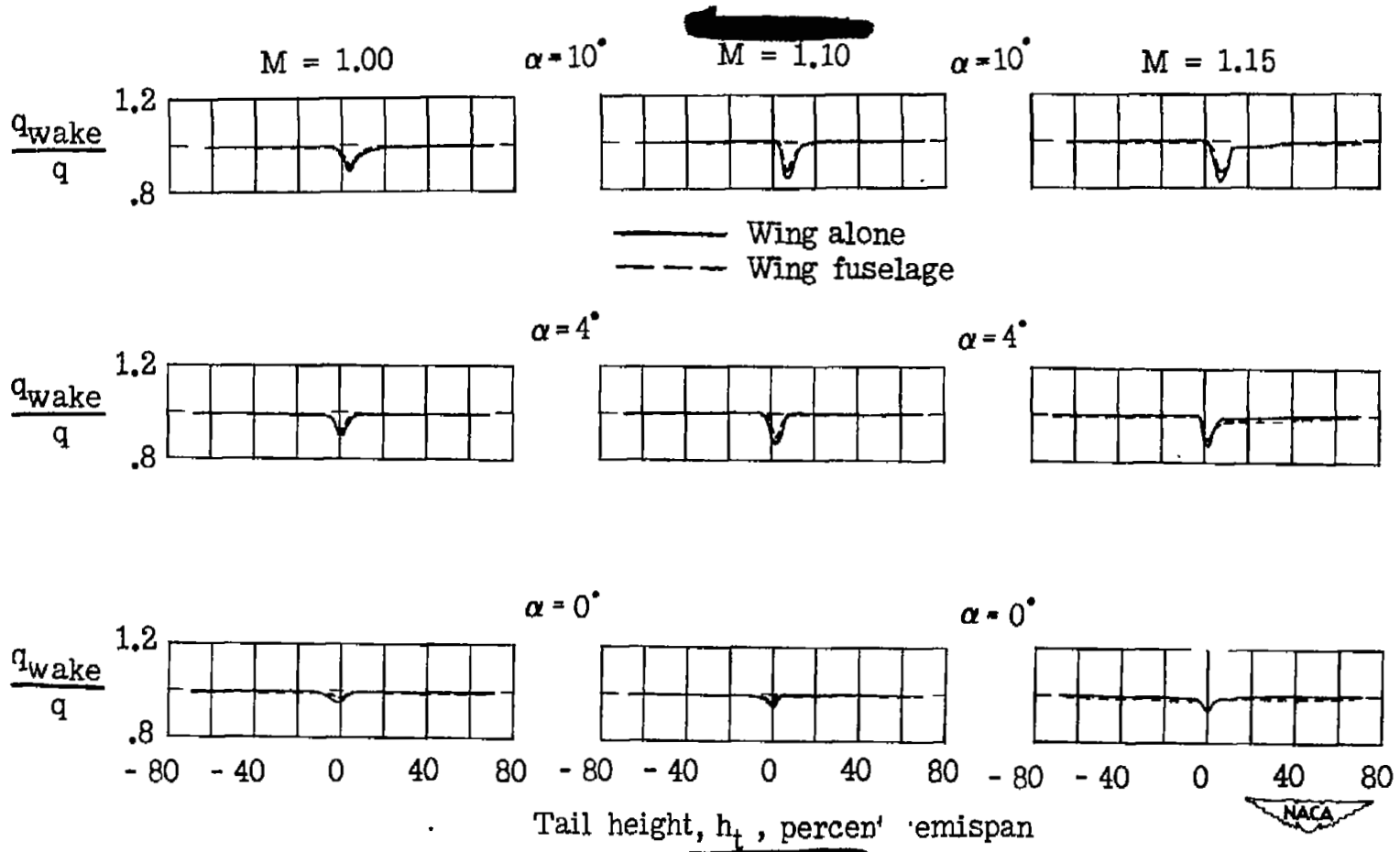




Figure 12.- Concluded.

 Wing alone
 Wing fuselage

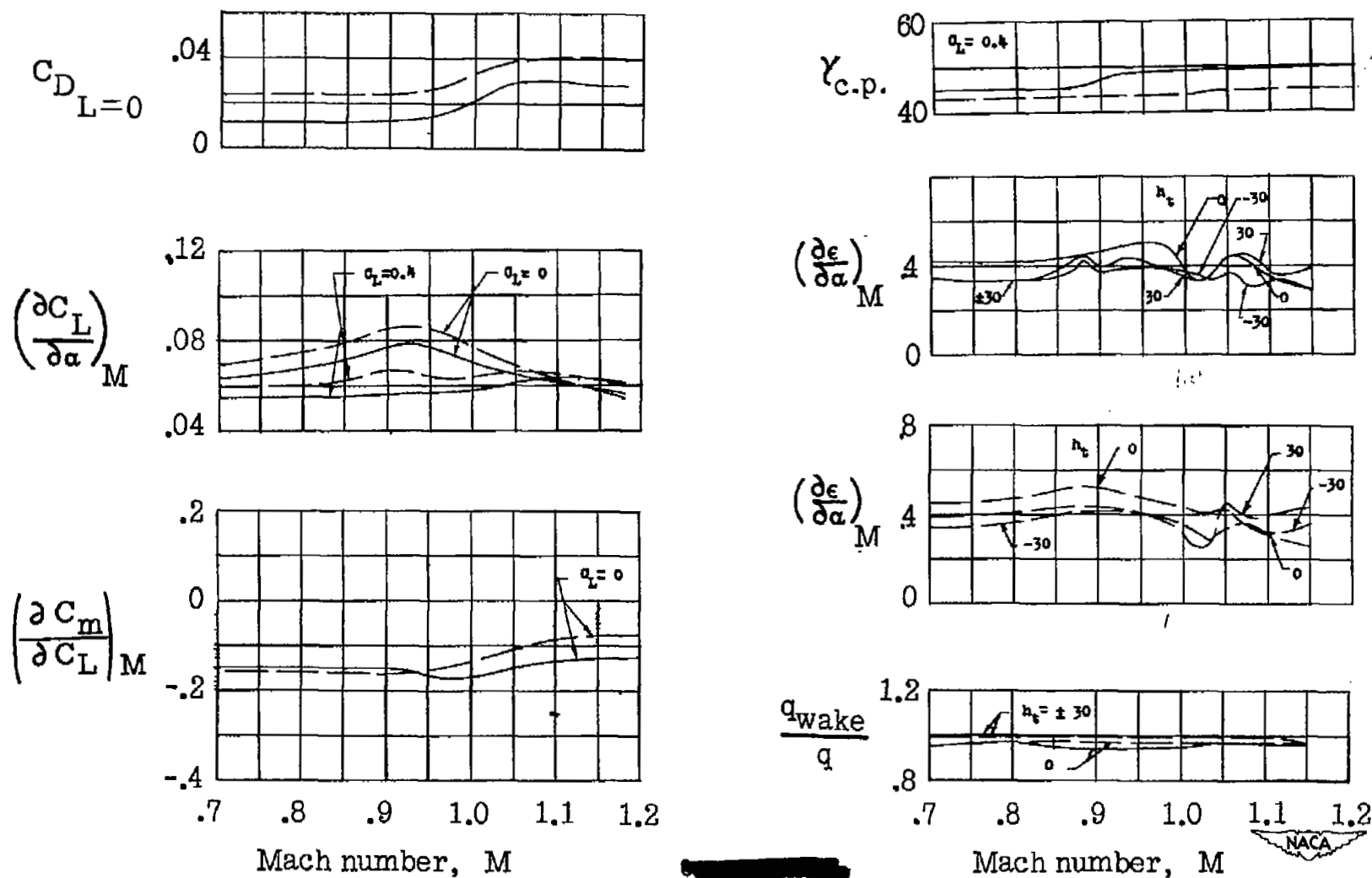


Figure 13.- Summary of aerodynamic characteristics for a model with 45° sweptback wing, aspect ratio 4, taper ratio 0.3, and NACA 65A006 airfoil.

NASA Technical Library



3 1176 01436 7503